Water-mediated conformer optimization in benzo-18-crown-6-ether/water system

*Ryoji Kusaka, Yoshiya Inokuchi, and Takayuki Ebata**

Department Chemistry, Graduate School of Science, Hiroshima University,

Higashi-Hiroshima 739-8526, Japan

Supporting Information

B18C6-$(H_2O)_4$ S10

Experimental

We used a home-made high temperature pulsed nozzle to generate supersonic jet of B18C6 and its hydrated clusters. The high temperature nozzle is made of a commercially available nozzle (General Valve series 9) and a sample housing made of poly-imido resin. B18C6 powder (Tokyo Kasei Kogyo) in the housing was heated to ~400 K. The gaseous mixture of B18C6 and water vapor, which was diluted by He carrier gas at the total pressure of 2 bar, was expanded into vacuum through 1 mm aperture. Partial pressure of water vapor was controlled by regulating the temperature of a water container connected to the gas line.

Electronic spectra were obtained by laser induced fluorescence (LIF) and mass-resolved resonance enhanced multiphoton ionization spectroscopy (REMPI). For the LIF measurement, an output of a pulsed UV laser (Inrad, Autotracker III (KDP) / Lambda Physik, Scanmate / Continuum, Surelite II) was introduced to the vacuum chamber at ~30 mm downstream of the nozzle. The LIF spectra were obtained by monitoring the total fluorescence as a function of UV frequency. Isomer-specific electronic spectra were obtained by UV-UV hole-burning spectroscopy. In this spectroscopy, two laser beams are used; pump and probe beams. The frequency of the probe UV laser is fixed to an origin band of a specific species and the fluorescence signal was monitored. A pump UV laser (Inrad, Autotacker II (KDP)/ Continuum, ND6000/ Continuum, Surelite II) is introduced to the jet at ~10 mm upstream of the probe laser beam. The pump light is introduced ~4 μs prior to the probe one. When the pump laser frequency is resonant to a transition of the monitored species, the species is excited to the upper state, resulting in a depletion of the fluorescence signal monitored by the probe light. Thus, the electronic spectrum of the monitored species is obtained as fluorescence dip spectra as a function of the pump UV frequency. The experimental scheme for obtaining infrared spectra by IR-UV double-resonance (IR-UV DR) spectroscopy is similar to that of UV-UV hole-burning spectroscopy. An output of a tunable IR laser (Laser Vision/ Quanta-Ray, GCR250) was introduced coaxially with the UV probe laser with its frequecny fixed to an origin band. The IR laser is ~100 ns prior to the probe UV. The frequency of the IR pump laser is scanned while monitoring the fluorescence signal. Depletion of the fluorescence occurs when the IR frequency is resonant to a vibrational transition of the monitored species. Thus, the IR spectrum in the S_0 state is obtained as fluorescence dip spectra.

In case of mass-resolved REMPI, the supersonic jet is skimmed by a skimmer before entering a time-of-flight mass spectrometer (TOFMS). The neutral species is photoionized by two-color REMPI, where the ionization laser is a third harmonic of another Nd:YAG laser (Surelite II). The ions are introduced to TOF tube and are detected by a channeltron. The ion signal is monitored by a digital oscilloscope and processed by a boxcar integrator.

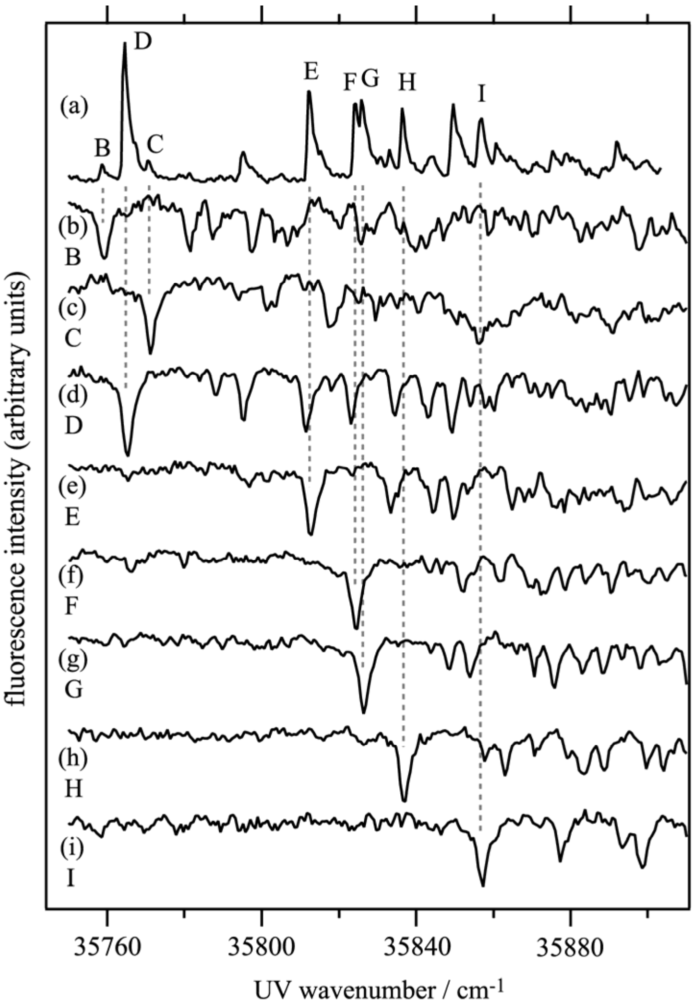

Figure S-1. (a) LIF of B18C6-$(H_2O)_n$ and (b-i) UV-UV hole-burning spectra of bands B-I in the 35750-35900 cm^{-1} region.

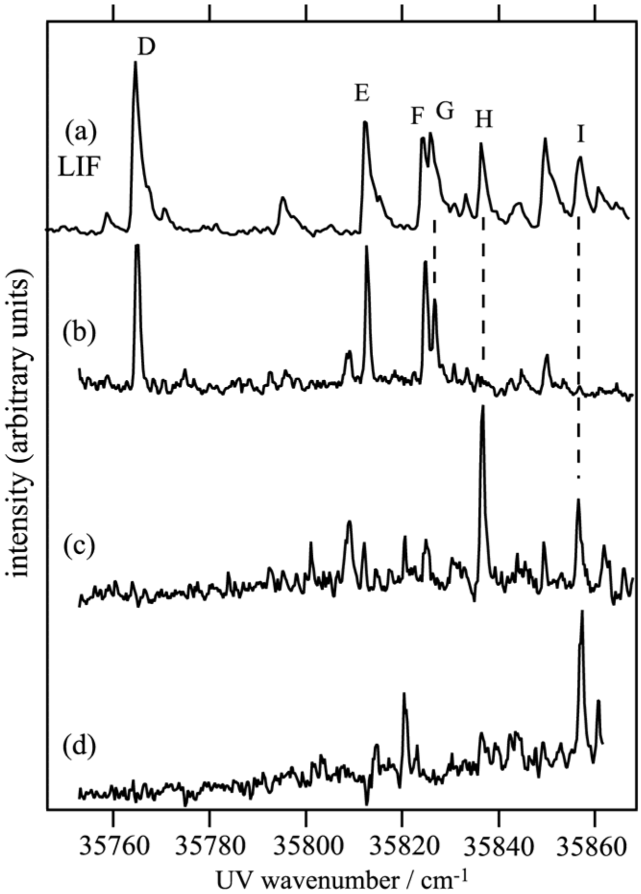

Figure S-2. (a) LIF spectrum of B18C6-$(H_2O)_n$ and (b-d) mass-resolved REMPI spectra observed by monitoring the mass channel of B18C6-$(H_2O)_m$ with m = 1-3, respectively. Species E-G, H, and I are assigned to B18C6-$(H_2O)_n$ with n=2, n=3, and n=4, respectively, in the text. The clusters lose one water molecule upon the ionization so that $n = m+1$.

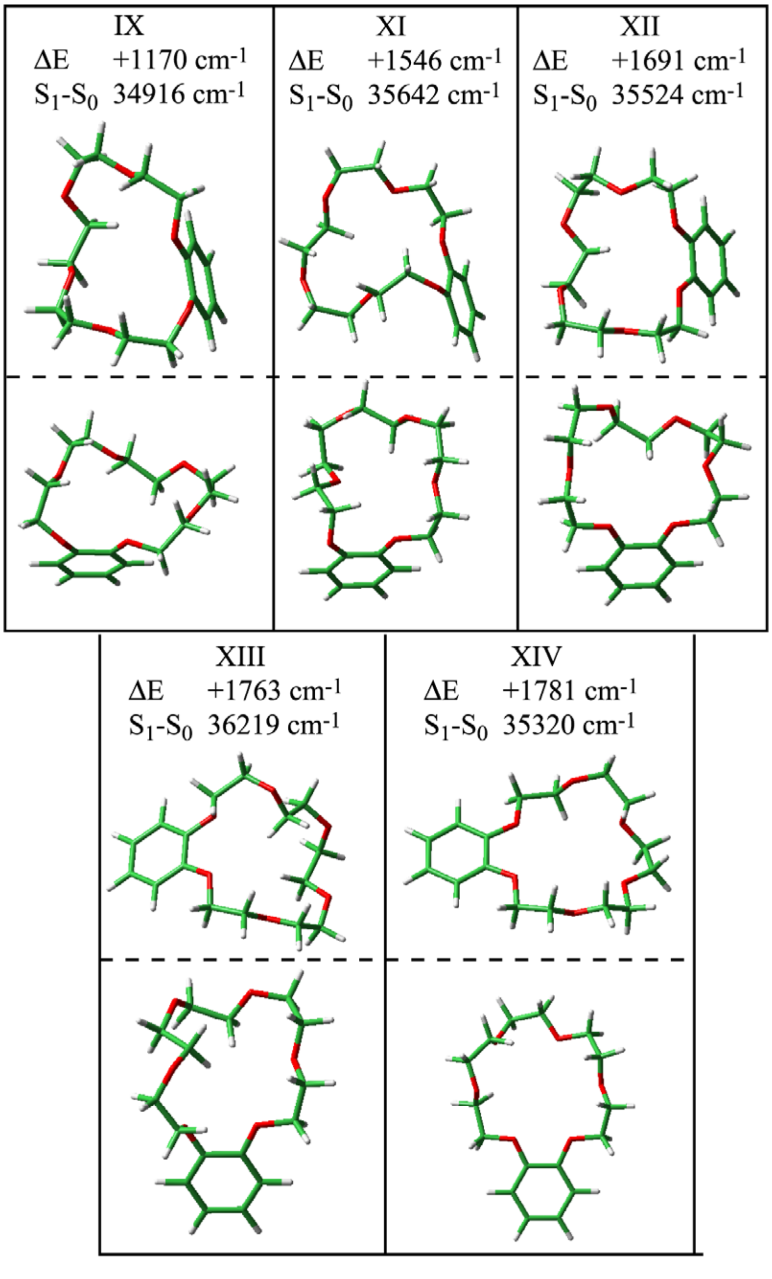

Figure S-3. Energy optimized conformers IX, XI-XIV calculated at B3LYP/6-31+G* level. ΔE is the energy relative to that of conformer I. S_1-S_0 is the scaled electronic transition energy obtained by TDDFT method at the B3LYP/6-31+G* level.

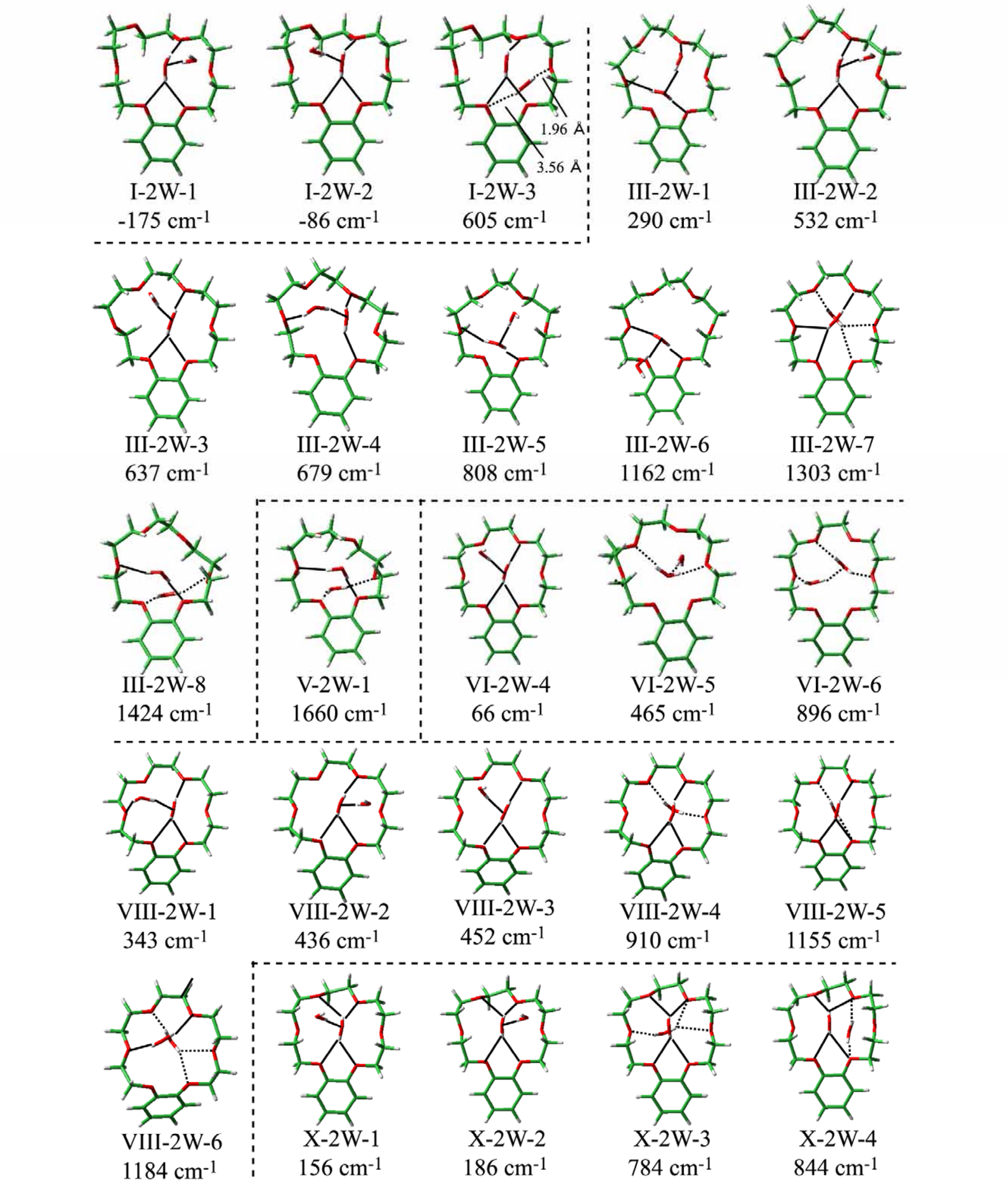

I-2W-1 -175 cm^{-1}
I-2W-2 -86 cm^{-1}
I-2W-3 605 cm^{-1}
III-2W-1 290 cm^{-1}
III-2W-2 532 cm^{-1}
III-2W-3 637 cm^{-1}
III-2W-4 679 cm^{-1}
III-2W-5 808 cm^{-1}
III-2W-6 1162 cm^{-1}
III-2W-7 1303 cm^{-1}
III-2W-8 1424 cm^{-1}
V-2W-1 1660 cm^{-1}
VI-2W-4 66 cm^{-1}
VI-2W-5 465 cm^{-1}
VI-2W-6 896 cm^{-1}
VIII-2W-1 343 cm^{-1}
VIII-2W-2 436 cm^{-1}
VIII-2W-3 452 cm^{-1}
VIII-2W-4 910 cm^{-1}
VIII-2W-5 1155 cm^{-1}
VIII-2W-6 1184 cm^{-1}
X-2W-1 156 cm^{-1}
X-2W-2 186 cm^{-1}
X-2W-3 784 cm^{-1}
X-2W-4 844 cm^{-1}

Figure S-5. Calculated structures B18C6-$(H_2O)_2$ which are not shown in the article. The energies of the isomers are given relative to that of VI-2W-3. In I-2W-3, the OH---O_1 and OH---O_{13} distances are shown in Å unit. The value of 3.56 Å is too long to be regarded as the H-bonding distance, indicating that conformer I can not incorporate two water molecules with a bidentate manner.

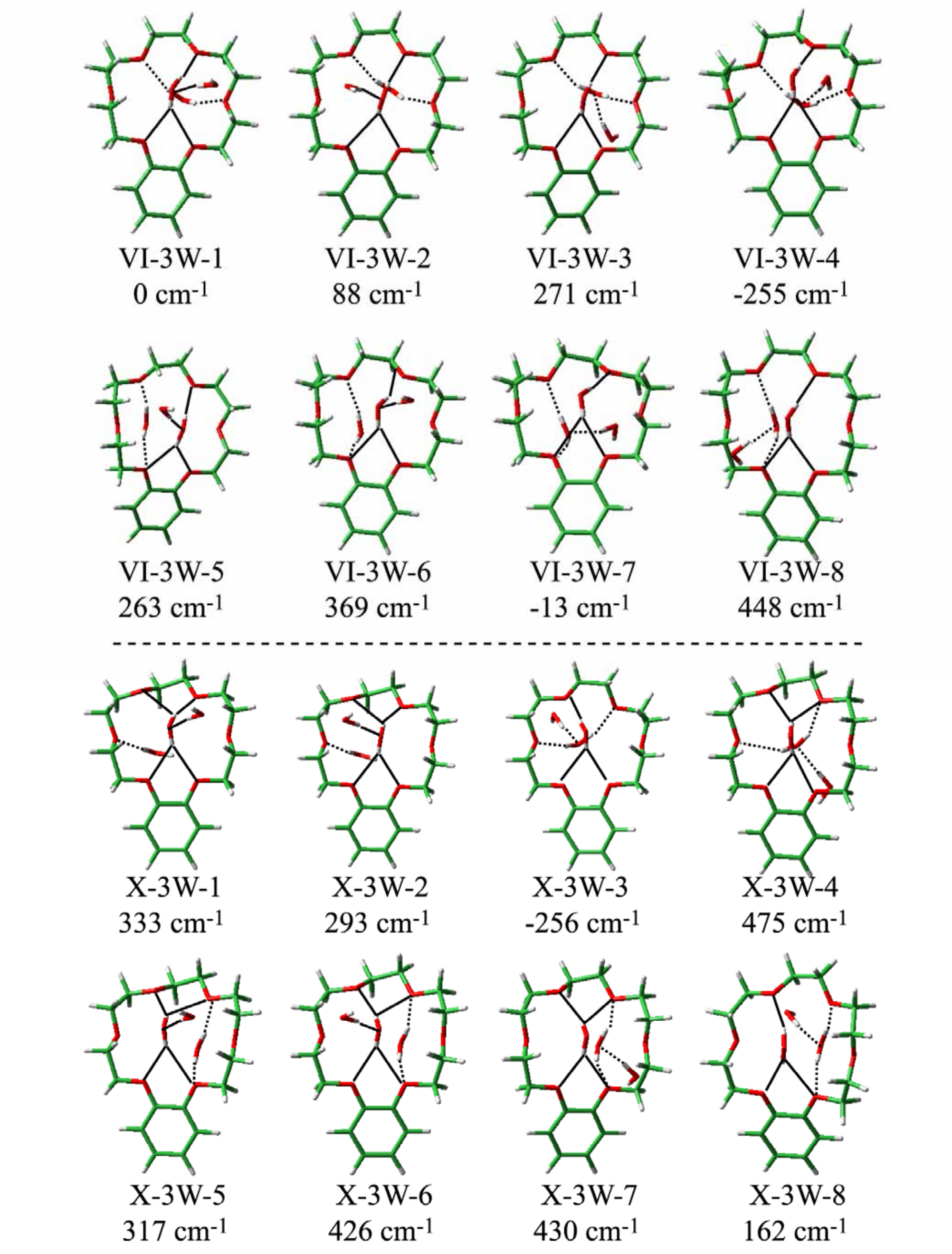

VI-3W-1 0 cm^{-1}
VI-3W-2 88 cm^{-1}
VI-3W-3 271 cm^{-1}
VI-3W-4 -255 cm^{-1}
VI-3W-5 263 cm^{-1}
VI-3W-6 369 cm^{-1}
VI-3W-7 -13 cm^{-1}
VI-3W-8 448 cm^{-1}
X-3W-1 333 cm^{-1}
X-3W-2 293 cm^{-1}
X-3W-3 -256 cm^{-1}
X-3W-4 475 cm^{-1}
X-3W-5 317 cm^{-1}
X-3W-6 426 cm^{-1}
X-3W-7 430 cm^{-1}
X-3W-8 162 cm^{-1}

Figure S-6. Calculated structures of B18C6-$(H_2O)_3$. Relative energies with respect to VI-3W-1 are shown.

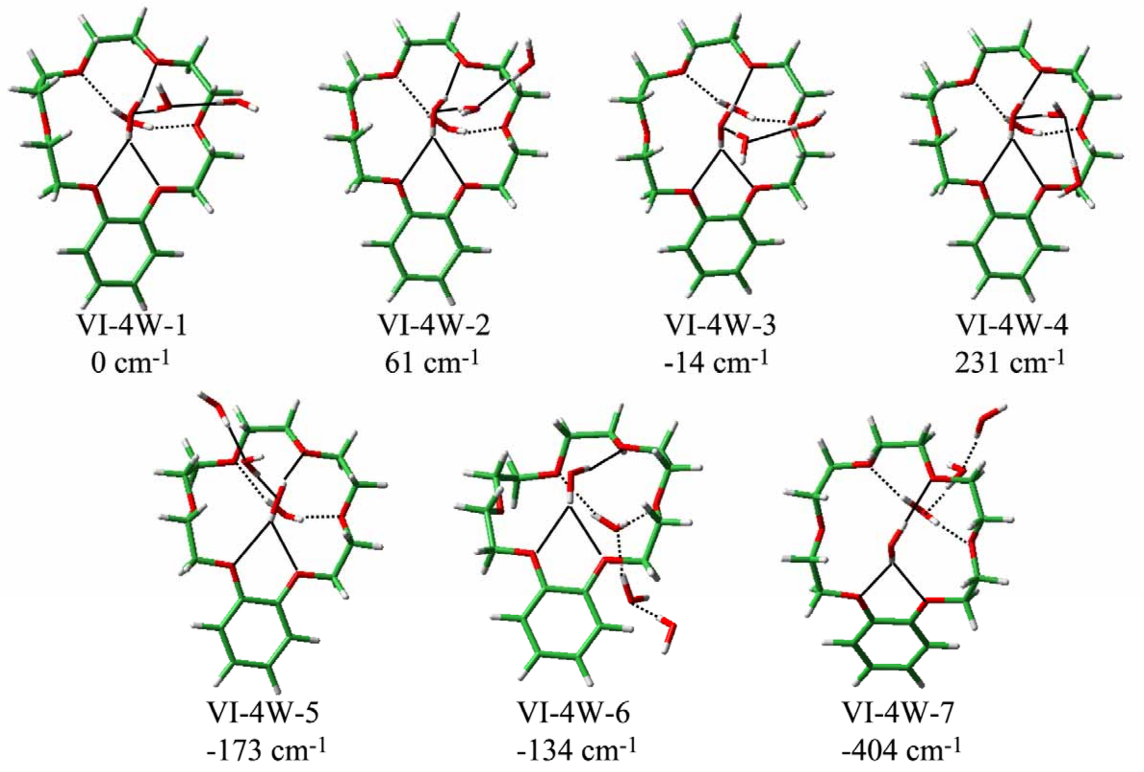

VI-4W-1
0 cm^{-1}

VI-4W-2
61 cm^{-1}

VI-4W-3
-14 cm^{-1}

VI-4W-4
231 cm^{-1}

VI-4W-5
-173 cm^{-1}

VI-4W-6
-134 cm^{-1}

VI-4W-7
-404 cm^{-1}

Figure S-7. Optimized structures of B18C6-$(H_2O)_4$. Their energies are given by relative energies with respect to that of VI-4W-1.